# CHAPTER 5
# EARTHQUAKE HAZARD ASSESSMENT

# *Chapter 5. Earthquake Hazard Assessment*

## 5-1 Scenario Earthquakes

### 5-1-1 Identification of Active Faults

Several regional structures identified in the Algiers area are likely to be reactivated within the present-day stress pattern.

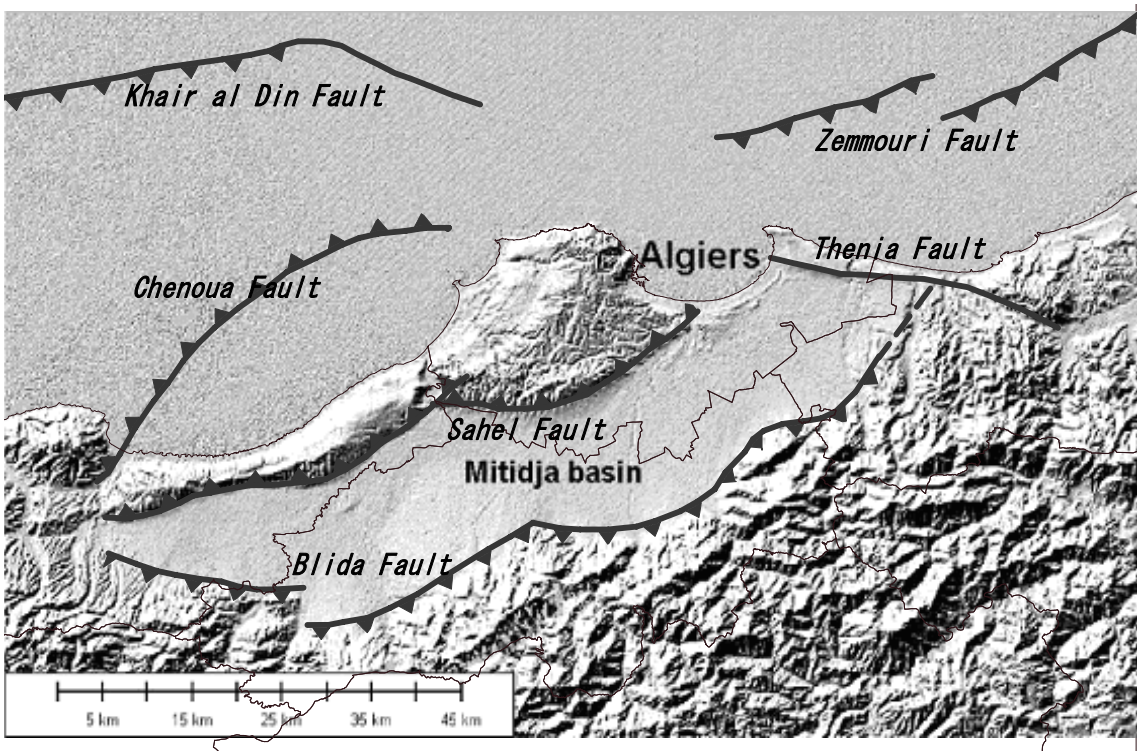


Background Image: SRTM DEM

Figure 5-1 Location and Inferred Surface Traces of Faults

(1) Sahel Fault

The Sahel fault forms the boundary between the Mitidja basin to the south and the Sahel of Algiers to the north (Figure 5-1). The topography following the fault on its northern compartment is an ENE-WSW trending anticline of about 200 m elevation, which results from reverse slip on the north-dipping fault plane. The Sahel fault does not propagate to the surface and remains blind along its entire length.

Two major segments are identified on the DEM, which connects at the Oued Mazafran. The eastern segment appears as a southward propagation of thrusting and accommodates some deformation that was likely to have been previously located on a now abandoned northern segment. Numerous data were published documenting the plioquaternary activity of the fault (e.g. Glangeaud, 1952; Aymé, 1952 ; Saoudi, 1989; Boudiaf, 1996), although the sharp and well preserved topography of the Sahel anticline, along with instrumental seismicity, themselves suggest active displacement along the fault.

(2) Chenoua Fault

The Chenoua fault bounds the Chenoua massif to the south and extends offshore in a northeast direction (Figure 5-1). Because this fault is offshore along most of its length, its precise geometry is poorly documented. However, two recent earthquakes on October 29, 1989 (Chenoua earthquake, Ms = 6.0) and February 9, 1990 (Tipaza earthquake, Ms = 4.9) yielded crucial information on the fault geometry. Aftershocks from these two events suggested two parallel fault planes, striking NE-SW and dipping approx. 45° to the NW (Maouche, 2000). These two planes are considered to merge at depth and form a single fault. In addition, focal mechanisms from these two earthquakes confirm purely reverse faulting on fault planes dipping approximately 45° towards the northwest (Figure 3-9). A reflection seismic profile across the fault shows a growing anticline on the northwestern fault compartment suggesting that for the Chenoua fault a geometry-associated topography closely similar to the Sahel fault.

Recently, the MARADJA scientific cruise offshore of the Algerian coast crossed the surface trace of the Chenoua fault several times allowing precise measurement of its extension (Domzig et al., submitted). Bathymetric data show a fault trace that extends for about 50 km to the west of Ain Benian. Considering the geometry of the Chenoua fault, it is likely that the Ain Benian earthquake of September 4, 1996 (Ms = 5.7), whose focal mechanism (GFZ) shows reverse motion on a northwestward dipping fault plane (Figure 3-9), was generated by this active structure.

(3) Blida Fault

The Blida (south Mitidja) Fault marks the boundary between the Mitidja basin to the north and the Blidean Atlas to the south (Figure 5-1). The Blidean Atlas is a range of steep topography with an elevation of approximately 1500 m. This topography reflects long-term reverse displacement on the south dipping fault plane. Well-developed superimposed fans in the piedmont of the range assert its recent to present uplift.

The surface trace of the fault appears segmented in the topography. Its deep geometry and segmentation, however, are not known. At its western termination, the fault trace progressively fades out before connecting to either the Sahel fault or the Tipaza fault. On its eastern termination, the fault trace also fades out and its topographic signal disappears before reaching the Boumerdes area (blind faulting?).

Instrumental seismicity shows a strong seismic activity, mostly focused on the western part of the fault (Figure 3-8). The Oued Djer earthquake of October 31, 1988 (Ms = 5.4) confirms reverse motion on a south dipping fault plane, with an additional right-lateral component of displacement (Figure 3-9).

(4) Offshore Active Faulting along the Algerian Margin

The Boumerdes earthquake of May 21, 2003 casts new light on the tectonic framework of the Algiers area. Studies of the main shock and subsequent aftershocks (Bounif et al., 2004 ; Delouis et al., 2004 ; Yelles et al., 2004) revealed that the earthquake occurred along a N55E to N60E-striking fault plane dipping 45° to 55° southeastward, offshore from Zemmouri. The focal mechanism of the main shock shows purely reverse slip. Recent offshore bathymetric and seismic reflection data from the MARADJA cruise (Deverchères et al., 2005)

image the trace of this offshore fault along the base of the continental slope north of Zemmouri (Figure 5-2). Activity along this fault could not be questioned, as evidenced by: 1) the recent Boumerdes earthquake and 2) fan-like geometry of quaternary sediments at the base of the continental slope (Figure 5-3).

Bathymetric data from the MARADJA cruise show a westward extension of this Zemmouri offshore fault not farther than the approximate longitude of Cape Matifou. However, additional data from the MARADJA cruise, west of the Algiers Bay (Domzig et al., submitted), show a similar major south dipping offshore fault following the base of the continental slope north of the Khair al Din bank (Figure 5-4). Bathymetric data show an eastward extension of this fault to the approximate longitude of Ain Benian. Even though there is no bathymetric evidence to show eastward extension of the fault trace to the Algiers Bay, we consider that this Khair al Din offshore fault should extend at depth beneath at least part of the Study Area.

According to the topographic signal (approximately 2,500 m of continental slope), these Zemmouri and Khair al Din offshore faults (Figure 5-1) have to be considered as major active structures. In this context the Sahel and Chenoua faults, which account for topographies of several hundred meters, are secondary structures, i.e. backward reverse faults (backthrusts) on the upper compartment of the Khair al Din offshore fault.

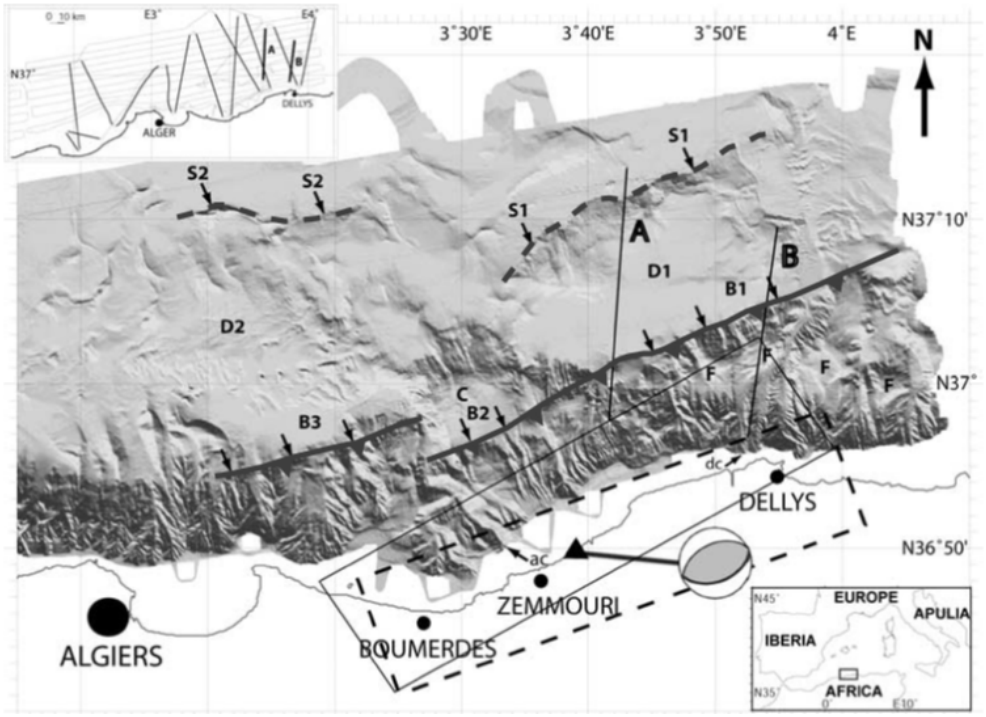


Figure 5-2 Bathymetric Data from the Maradja Ccuise (eastern part), showing the Zemmouri offshore fault that generated the May 21, 2003 Boumerdes earthquake (modified from Deverchères et al., 2005)

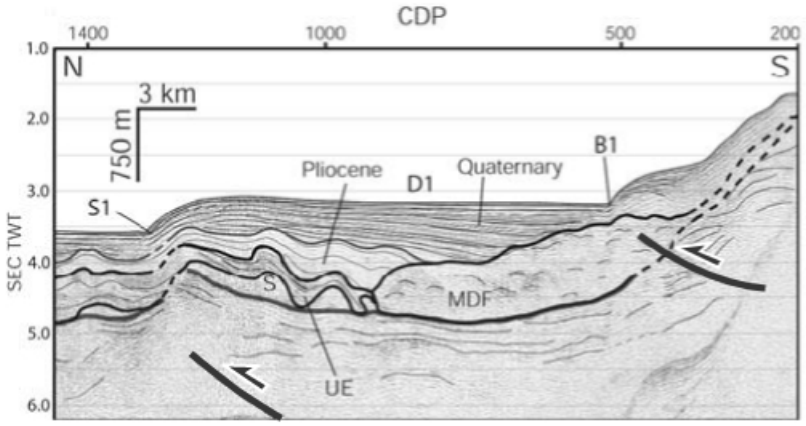


Figure 5-3 Reflection Seismic Data from the Maradja Cruise showing quaternary deposits tilted by displacement along the offshore fault that generated the May 21, 2003 Boumerdes earthquake (modified from Deverchères et al., 2005)

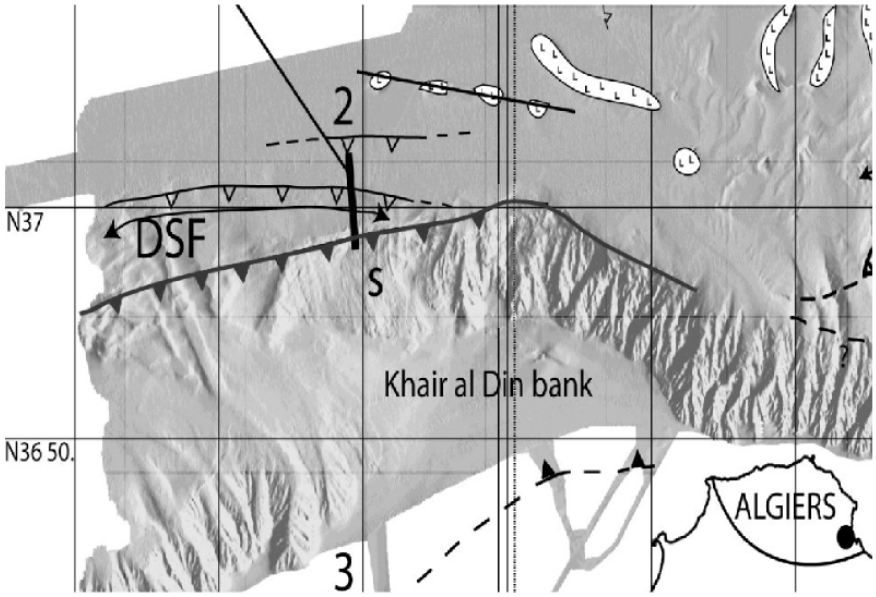


Figure 5-4 Bathymetric Data from the MARADJA Cruise (western part), showing the Khair al Din offshore fault north of Khair al Din bank (modified from Domzig et al., submitted)

(5) Thenia Fault

The Thenia fault runs in a WNW-ESE direction near the Boumerdes city. It extends from the Algiers Bay to the Oued Isser over a total length of approximately 35 km (Figure 5-1). Recently published bathymetric data do not show a significant offshore extension of the fault (Deverchères et al., 2005). The fault trace in the topography is rectilinear, which suggests a steeply dipping fault plane. The fault near the coastline forms a sharp topography of approximately 50 - 80 m elevation, which shows recent activity limited to uplift of the northern compartment.

### 5-1-2 Field Analyses

The purpose of field analyses is to precisely study the geometry and seismogenic capability of active faults identified by analyzing deformations of Quaternary sediments and/or perturbations of the morphology. The quantification of quaternary displacements is based on the measurement of offset of stratigraphic and/or morphological markers. In coastal areas such as the Algiers region, the study of quaternary marine terraces provides data on the amount and velocity of vertical displacements. These field analyses yield information on the seismogenic capability of active faults: geometry, velocity and, whenever possible, co-seismic vector and return period of major earthquakes.

(1) Activity along Sahel Fault

Traces of activity along the Sahel fault were investigated along the Oued Mazafran, which crosses the Sahel anticline south of Zeralda. In this area, the anticline was investigated along its entire width from the Mitidja basin to the sea.

No surface extension of the Sahel fault has been observed, although numerous minor surface deformations in quaternary deposits can be seen. These minor surface deformations are most probably gravity adjustments to the fault-driven topographic growth as they show both reverse and normal small-scale displacements. The topography by itself, either observed on a Digital Elevation Model, or in the field, is a sufficient argument to assert quaternary tectonic activity along the Sahel fault.

Abrasion marine terraces on the back limb of the Sahel anticline qualitatively confirm late Pleistocene (Tyrrhenian or younger) uplift due to slip on the fault. This observation should be quantified with detailed absolute dating and elevation profiles.

(2) Faulting in the Bouzareah Massif

The Bouzareah massif is located to the west of Algiers. It comprises metamorphic basement rocks and reaches a maximum elevation of approximately 400 m. Two faults have been described in this massif (Saadallah, 1981, 1984; Slemmons et al., 1984) and both are considered to be possibly active. The published arguments for tectonic activity along these faults along with our own field observations and subsequent interpretation are outlined below.

1) Ain Benian Fault

The first possibly active structure in the Bouzareah massif is an E-W striking fault that would cross Algiers' harbor and extend westward along the Oued Beni Messous to its mouth in Ain Benian. Existence of this fault is only suggested for a short length in the Algiers area (Saadallah, 1984), but Swan et al. (1998) considered it as the westward extension of the Thenia fault and therefore as a critical seismogenic source. No other publication describes or locates the Ain Benian fault.

To check the existence of this fault, we observed the burdigalian deposits and basement metamorphics along the Frais Vallon road between El Biar and Bab El Oued. No E-W striking fault was observed in this area that would have confirmed the existence of the Ain Benian fault.

In the present stress pattern, an E-W striking active fault would necessarily have a vertical component of displacement that would generate an asymmetric topography. The topography of Oued Beni Messous between Cheraga and Ain Benian was checked both in the field and on the Digital Elevation Model. No asymmetry in the topography was observed that could suggest an E-W striking fault reactivated in the present-day stress pattern (Figure 5-5).

These observations led us to question the existence of the Ain Benian fault. If it were to exist and be active, the undetectable topographic signal would assert that the slip rate would be at least two orders of magnitude slower than along the Sahel fault (that is itself one order of magnitude slower than the Blida and offshore faults). This very slow velocity, combined with limited length, would make this structure negligible in terms of seismic hazard.

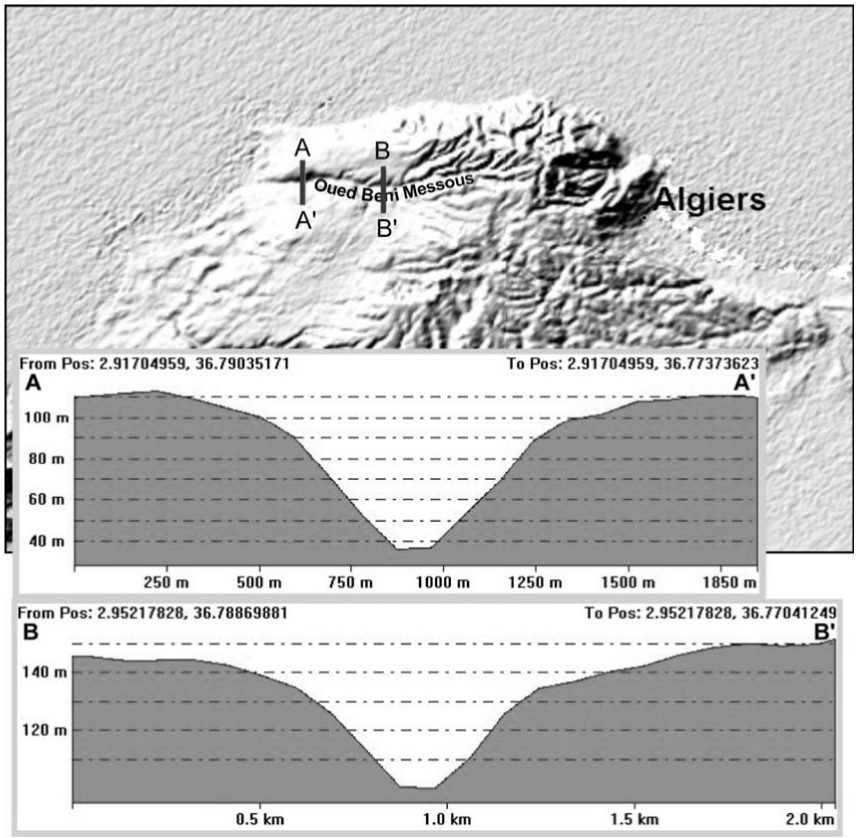


Figure 5-5 Topographic Profiles across Oued Beni Messous, showing lack of topographic asymmetry. Active faulting along the Oued would generate asymmetry of its banks in the present-day stress pattern

2) Bouzareah Fault

The second possibly active structure in the Bouzareah massif is an E-W striking reverse fault that would outcrop near Bains Romains (northern coast of the massif) but which has never been precisely mapped. This structure is “a reverse E-W striking fault, strongly dipping towards the south, in recent shallow formations” (translated from Saadallah, 1984, in French).

It should be noted, however, that "the faults near Bains Romains have not received careful exploration and evaluation" (Slemmons, 1984). We attempted to address this gap by observing possible recent deformation in quaternary deposits south of Bains Romains.

It was observed that in the wadi south of Bains Romains (road to Bouzareah), a small E-W striking reverse fault with basement metamorphics was possibly thrusting over quaternary colluvium by tens of centimeters (Figure 5-6). This observation is consistent with outcropping described by Saadallah (1981, 1984) except that he indicated the fault dips to the south while we observed it dipping to the north.

This suggests that the Bouzareah massif is cut by several E-W striking antithetic reverse faults, of very limited extension and slow slip rate. Such minor structures accommodate a very limited part of the deformation, which is mostly concentrated along major faults. They are negligible in terms of seismic hazard with regard to major sources nearby (offshore and Blida faults, or even the slower Sahel fault).

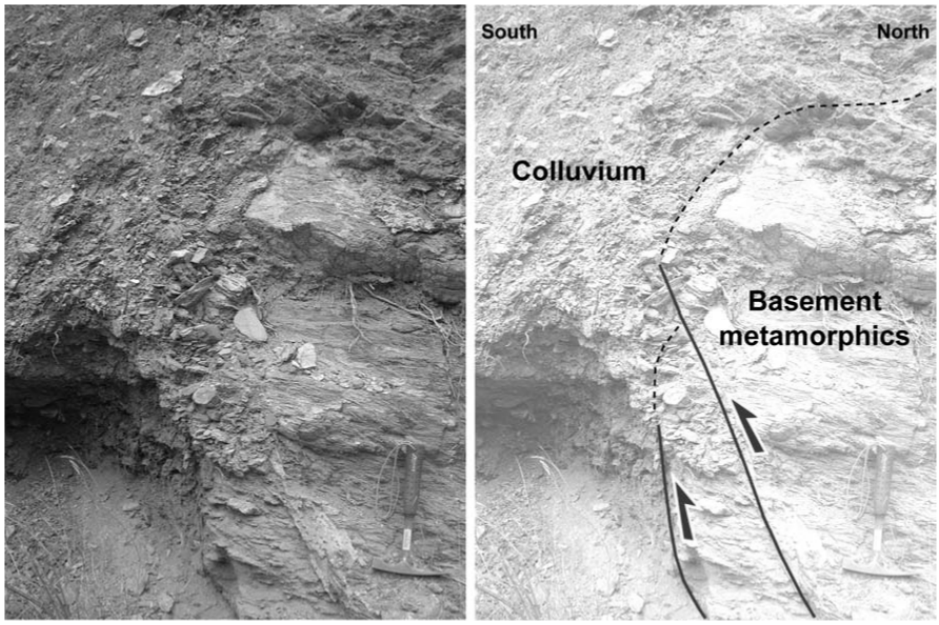


Figure 5-6 View of a Possible Minor E-W-striking North-dipping Reverse Fault Observed Near Bains Romains. This very minor structure would be similar to the fault described in the same area by Saadallah (1981, 1984)

### 5-1-3 Implementation of the Seismotectonic Model

(1) Seismotectonic Description of Individual Active Structures

Individual regional active structures previously identified, i.e. the Sahel, Blida, offshore and Thenia faults, are considered in terms of their seismotectonic impact within present-day patterns of deformation.

1) Sahel Fault

Despite numerous studies of the Sahel fault, its deep structure and geometry remain unknown. Critical information on fault geometry, such as angle of dip, segmentation and width of fault plane, are required to assess seismogenic capability and associated hazard. Nevertheless, as the deep geometry of the fault is not known, we consider a rupture along the entire fault length, i.e. approx. 75 km (with all segments merging at depth and rupturing together). We also consider that the Sahel fault extends downward to a depth of 15 km.

Detailed kinematics of the Sahel fault are also unknown. Based on radiometric age, Meghraoui (1991) calculated an uplift of marine terraces east of Tipaza of 0.1 to 0.2 mm/yr, although this uplift could result from accumulated slip on several structures (e.g. offshore fault). According to topographic response to displacement along the Sahel fault, it is estimated that slip rate should be in the order of a few tenth of mm per year. For this Study, a slip rate of 0.5 ± 0.2 mm/yr will be considered along the Sahel fault.

2) Chenoua Fault

According to bathymetric data from the MARADJA cruise and instrumental seismicity, it is considered that the Chenoua fault has an approximate length of 50 km and a northwest dip of 45°. If we consider that the response of the topography to displacement along the Chenoua fault is relatively comparable to the Sahel fault, similar slip rates could be considered along these two structures. Therefore, for this Study a slip rate of 0.5 ± 0.2 mm/yr will be assumed along the Chenoua fault.

3) Blida Fault

As for the Blida fault, significant uncertainties are associated with: 1) geometry at depth (angle of dip, downward propagation, segmentation, connection to other structures, …), and 2) velocity slip rate.

As segmentation at depth is not known, we will consider the Blida fault segments identified in the topography merge at depth and form a single segment with an approximate length of 90 km. It is also considered that the Blida fault extends to a depth of 20 km.

According to the topographic signals generated by both the Blida and the Sahel faults, it appears that velocity along the Blida fault is significantly faster than along the Sahel fault (1,500 m elevation versus 200 m, respectively). It is assumed that slip rate along the Blida fault could be one order of magnitude higher than along the Sahel fault, i.e. in the order of a few mm per year. Also, the Blida fault could at most accommodate about half the total Africa-Eurasia convergence. For this Study, a slip rate of 2.5 ± 1.0 mm/yr is therefore assumed along the Blida fault.

4) Offshore Active Faults along the Algerian Margin

Available bathymetric and reflection seismic data image the Zemmouri offshore fault in the eastern part of the Algiers area (Deverchères et al., 2005) and the Khair al Din offshore fault in the western part (Domzig et al., submitted). Segmentation for both

offshore faults is unknown, but a possible rupture along the entire length of each of these structures, i.e. approximately 100 km for the Zemmouri offshore fault and approximately 100 km for the Khair al Din offshore fault, is assumed. It is considered that these two major structures extend to a depth of 20 km.

According to the topographic signals generated by the offshore faults, when compared to the Blida fault, it appears that the slip rate is of the same order (2,500 m topography on the offshore faults, with lower submarine erosion rates, versus 1,500 m topography on the Blida fault, with higher aerial erosion rates). It is therefore considered the slip rate along the offshore faults could then be in the order of a few mm per year. Considering the situation of each offshore fault within the present-day pattern of deformation, we have:

- To the west, a shortening distributed mainly over two major structures, the Khair al Din and Blida faults;
- To the east, a shortening accommodated by one major structure, the Zemmouri offshore fault.

This suggests:

- As for the Blida fault, the Khair al Din offshore fault could accommodate, at the most, about half the total Africa-Eurasia convergence, i.e. a slip rate of 2.5 ± 1.0 mm/yr along the Khair al Din offshore fault;
- The Zemmouri offshore fault could potentially accommodate the largest part of the total Africa-Eurasia convergence, i.e. a slip rate of 4.0 ± 1.0 mm/yr along the Zemmouri offshore fault.

5) Thenia Fault

Relative orientation of the Thenia fault within the present-day stress pattern suggests that its displacement is a right-lateral strike-slip. Boudiaf (1996) lists 3 arguments providing evidence of right-lateral active displacement along the Thenia fault. The activity along the Thenia fault is not questioned, however, it is thought that dextral strike-slip motion is not the active sense of displacement along the fault. The reinterpretations of Boudiaf's (1996) observations are outlined below:

- Microtectonic measurements in the Thenia granodioritic massif show evidence of dextral motion. The granodiorites were dated based on the K-Ar method (Belanteur et al., 1995), yielding a Miocene age (18.5 to 22.5 Ma). Observed strike-slip displacements are then post-burdigalian (lower Miocene), i.e. they might have occurred any time between 18.5 Ma and the present;
- Secondary streams of the hydrographic network show z-like shapes as they cross the fault. This geometry has been considered to result from right-lateral displacement along the stream. It could, however, also result from capture of streams resulting from vertical displacement of the northern block;
- Geometry of the Oued Isser, as well as fluvial terraces, show that its downstream course has deviated eastward along the fault trace. This could not result from right-lateral displacement on the fault as it would require 5 to 7 km of horizontal offset on a 35 km long fault. We consider that such a horizontal slip, moreover

concentrated on its termination, is mechanically not possible on a fault of this length. As a consequence, eastward deviation of the downstream course of the Oued Isser is more likely to result from differential vertical displacement of fault compartments.

We therefore suggest that the Thenia fault accommodates differential vertical and limited horizontal displacement between i) a northeastern block, where shortening is concentrated on one single fault (Zemmouri offshore fault), and ii) a southwestern block, where shortening is distributed over two faults (Khair al Din offshore and Blida faults). The Mitidja basin is then a "piggy-back" basin carried on the back of the Khair al Din offshore thrust.

If displacement along the Thenia fault is vertical with relative uplift of the northern compartment, with regard to the topographic signal we can only consider a very limited slip rate.

For the reasons presented above it is considered the Thenia fault is a secondary structure with regards to its length and role in the regional tectonic context (it does not accommodate shortening, but rather differential vertical displacements). For this Study, a slip rate of 0.75 ± 0.25 mm/yr along the Thenia fault is therefore assumed. This value appears rather conservative given the present state of knowledge.

(2) Seismotectonic Model

Critical analysis of all available data (geodynamics, tectonics, geology, seismicity, morphology, remote sensing, and so on) allows for implementing a new seismotectonic model in the light of the understanding of the 2003 Boumerdes earthquake.

For Algiers seismic hazard, this results in six critical faults (Figure 5-7):

- The known north dipping Sahel thrust bounding the Mitidja basin to the north;
- The northwest dipping Chenoua that extends offshore and is similar, from the seismotectonic aspect, to the Sahel fault;
- The known south dipping Blida thrust bounding the Mitidja basin to the south;
- A new major south dipping Zemmouri offshore thrust located at the foot of a 2,500 m high north-facing offshore scarp east of the Algiers Bay;
- A new major south dipping Khair al Din offshore thrust located at the foot of a 2,500 m high northwest-facing offshore scarp west of the Algiers Bay;
- The already known Thenia fault that bounds two blocks and accommodates their differential displacement.

Within that framework, the Thenia fault is given a less important role than in previous models (e.g. Swan et al., 1998) as it only accommodates the differential displacement between the Zemmouri block to the northeast (only one thrust absorbing the shortening) and the Algiers block to the southwest (2 major thrusts absorbing the shortening with a superimposed subsiding Mitidja basin). As 1) bathymetric data does not show any evidence of an offshore extension, and 2) a southern extension of this fault, south-east of the Oued Isser right bank, is neither visible in geology or topography, we do not consider that given the present state of

knowledge the Thenia fault is a major regional tectonic structure. One should, however, keep in mind that despite the minor role assigned to the Thenia fault in our seismotectonic model, it is still an active structure able to generate strong earthquakes.

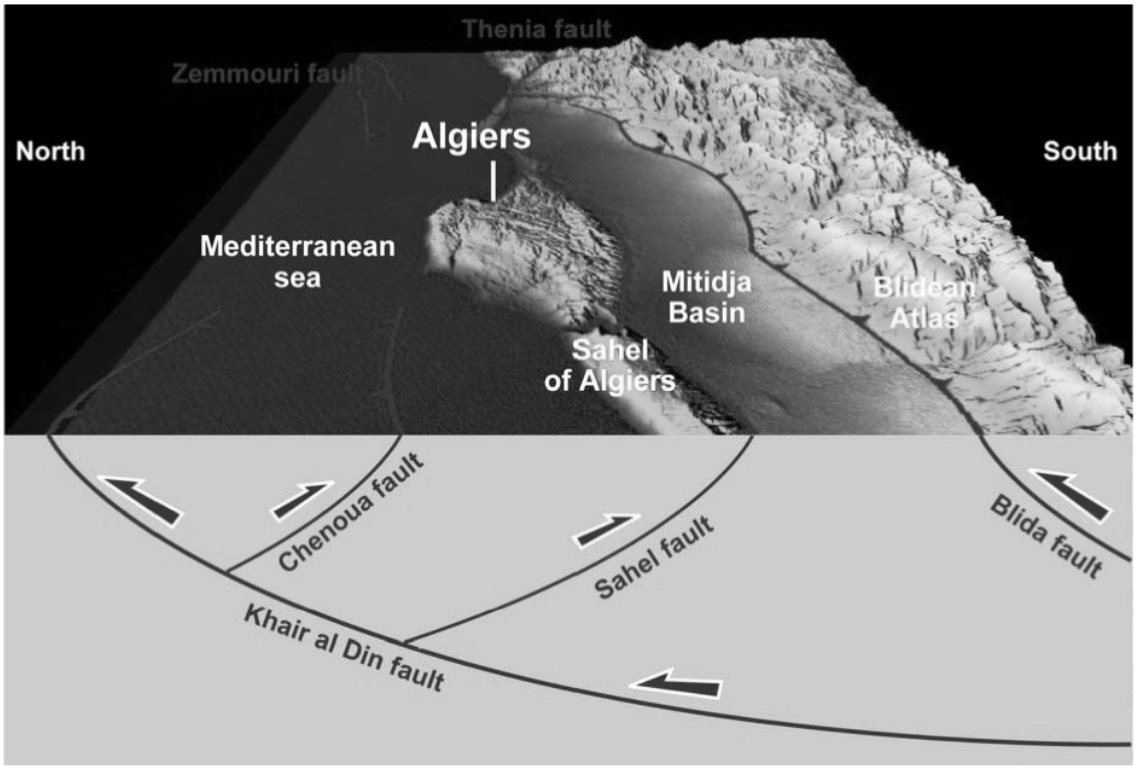


Figure 5-7 Block Diagram Showing 3D Geometry of the Proposed Seismotectonic Model

### 5-1-4 Seismogenic Capabilities of the Faults

(1) Maximum Credible Earthquake (MCE)

1) Methodology

A maximum magnitude (Maximum Credible Earthquake, MCE) has to be assigned to each identified critical seismogenic source, i.e. faults capable of representing a threat to the Study Area. This is the largest reasonably conceivable earthquake that appears possible along a recognized fault, under the presently known or presumed tectonic framework. Several methods for estimating the maximum magnitude are discussed in detail by Idriss (1985). The capability of these faults should have been ascertained through historical and instrumental seismic data and geological criteria such as the rupture length-magnitude, rupture-area-magnitude, slip-vector-magnitude, slip-rate-magnitude and seismic moment-magnitude relationships.

Recently, the use of seismic moment has provided a physically meaningful measurement of the size of a faulting event. Seismic moment (Mo), in dyne-cm, is expressed by the equation:

$$Mo = \mu \cdot A_f \cdot D$$

in which μ is the shear modulus of the material along the fault plane, typically equal to 3 x $10^{11}$ dyne/cm$^2$ for crustal rocks, Af is the area, in cm$^2$, of the fault plane undergoing slip, and D, in cm, is the average displacement over the slip surface. Seismic moment provides a basic link between the dimensions of the fault and the seismic waves radiated due to rupturing along the fault. Seismic moment is therefore more reliable than the other methods. Kanamori (1977) and Hanks and Kanamori (1979) introduced a moment-magnitude scale, Mw, in which magnitude is calculated from seismic moment using the following formula:

$$\log_{10} Mo = c \cdot Mw + d$$

The moment-magnitude differs from other magnitude scales because it is directly related to average slip and ruptured fault area, while the other magnitude scales reflect the amplitude of a particular type of seismic wave.

The MCE on each identified active fault is derived using relationships from Wells & Coppersmith (1994). They compiled worldwide surface breaks related to earthquakes and derived empirical relationships between the seismic moment and the geometry of the rupturing fault plane (fault length, fault width, area of rupture, etc.).

For reverse faults, these relationships are:

$$Mw = 5.00 + 1.22 \cdot \log_{10} SRL \pm 0.28$$
$$Mw = 4.49 + 1.49 \cdot \log_{10} RL \pm 0.26$$
$$Mw = 4.37 + 1.95 \cdot \log_{10} RW \pm 0.32$$
$$Mw = 4.33 + 0.90 \cdot \log_{10} RA \pm 0.25$$

and for strike slip faults:

$$Mw = 5.16 + 1.12 \cdot \log_{10} SRL \pm 0.28$$
$$Mw = 4.33 + 1.49 \cdot \log_{10} RL \pm 0.24$$
$$Mw = 3.80 + 2.59 \cdot \log_{10} RW \pm 0.45$$
$$Mw = 3.98 + 1.02 \cdot \log_{10} RA \pm 0.23$$

where SRL is the surface rupture length in km, RL is the subsurface rupture length in km, RW is the down dip rupture width in km, and RA is the rupture area in km$^2$.

Because the area of rupture is the best-defined parameter of the ruptured plane geometry (it combines subsurface length and down dip width, which itself combines dip and depth), we have applied the latter relationships, that is between moment magnitude and area of rupture. The strike slip fault relationship is used for the Thenia fault while the reverse fault relationship is used for the remaining five faults.

2) MCE of Seismogenic Structures in the Algiers Area

Based on the present knowledge of seismotectonics, the Maximum Credible Earthquake (MCE) for identified active faults in the Algiers area is given in the following sections. These values are summarized in Table 5-1 below.

(A) Sahel Fault

For the Sahel fault, the MCE has been derived from its segmentation as deduced from a Digital Elevation Model (SRTM) and satellite image. Assuming a 75 ± 10 km long fault dipping 45° northward to a depth of 15 km where it connects to the antithetic offshore fault, the seismogenic capability of this source is:

$$Mw = 7.2 \pm 0.3$$

which corresponds to a rupture area of 1590 ± 210 km$^2$.

(B) Chenoua Fault

For the Chenoua fault, the Maximum Credible Earthquake has been derived from the geometry of the fault plane, as imaged by the distribution of aftershocks from the Chenoua (29/10/1989, Ms=6.0) and Tipaza (09/02/1990, Ms=4.9) earthquakes (Maouche, 2000). Assuming a 50 ± 10 km long fault dipping 45° northwestward to a depth of 15 km, the seismogenic capability of this source is:

$$Mw = 7.0 \pm 0.3$$

which corresponds to a rupture area of 1060 ± 210 km$^2$.

(C) Blida Fault

For the Blida fault, the Maximum Credible Earthquake has been derived from its segmentation as deduced from a Digital Elevation Model (SRTM) and satellite image. Assuming a 90 ± 10 km long fault dipping 45° southward to a depth of 20 km, the seismogenic capability of this source is:

$$Mw = 7.4 \pm 0.3$$

which corresponds to a rupture area of 2545 ± 280 km$^2$.

(D) Khair al Din Fault

For the Khair al Din offshore fault, the Maximum Credible Earthquake has been derived from its segmentation and downdip geometry of the fault plane, as imaged by offshore data from the MARADJA cruise (Deverchères et al., 2005). Assuming a 100 ± 20 km long fault dipping 45° southward to a depth of 20 km, the seismogenic capability of this source is:

$$Mw = 7.4 \pm 0.3$$

which corresponds to a rupture area of 2830 ± 565 km$^2$.

(E) Zemmouri Fault

For the Zemmouri offshore fault, the Maximum Credible Earthquake has been derived from its segmentation and downdip geometry of the fault plane, as imaged by offshore data from the MARADJA cruise (Deverchères et al., 2005). Assuming a 100 ± 20 km long fault dipping 45° southward to a depth of 20 km, the seismogenic capability of this source is:

$$Mw = 7.4 \pm 0.3$$

which corresponds to a rupture area of 2830 ± 565 km$^2$.

(F) Thenia Fault

For the Thenia fault, the Maximum Credible Earthquake has been derived from its geometry as deduced from a Digital Elevation Model (SRTM) and satellite image. Assuming a vertical fault reaching a depth of 15 km and a length of 40 ± 10 km, the seismogenic capability of this source is:

$$Mw = 6.8 \pm 0.3$$

which corresponds to a rupture area of 600 ± 150 km$^2$.

Table 5-1 Seismic Capability (Magnitude of MCE) of Regional Active Faults

| Fault | Length (km) | Dip Angle (°) | Depth (km) | Rupture Area (km$^2$) | Mw |
|---|---|---|---|---|---|
| Sahel Fault | 75 ± 10 | 45 | 15 | 1590 ± 210 | 7.2 ± 0.3 |
| Chenoua Fault | 50 ± 10 | 45 | 15 | 1060 ± 210 | 7.0 ± 0.3 |
| Blida Fault | 90 ± 10 | 45 | 20 | 2545 ± 280 | 7.4 ± 0.3 |
| Khair al Din Fault | 100 ± 20 | 45 | 20 | 2830 ± 565 | 7.4 ± 0.3 |
| Zemmouri Fault | 100 ± 20 | 45 | 20 | 2830 ± 565 | 7.4 ± 0.3 |
| Thenia Fault | 40 ± 10 | 45 | 15 | 600 ± 150 | 6.8 ± 0.3 |

(2) Magnitude Versus Return Period

1) Methodology

A probabilistic approach does not seem pertinent to the Algiers area since earthquake sampling is very poor in terms of density, time frame and magnitude. Such an approach would result in a dilution of the hazard over large source areas.

A purely historical (deterministic) approach, implying the need to locate the Maximum Historical Earthquake at the more critical location along the fault, also does not seem pertinent because it would result in a very conservative hazard independent of any return periods.

We propose to mix probabilistic and deterministic approaches focussing on hazard controlled by identified active faults through models developed by Anderson (1979), Anderson and Luco (1983) and Youngs and Coppersmith (1985). The magnitudes for a given return period appropriate for urban planning are determined.

(A) Acceptable Risks

The mean return period, $T_m$, of an earthquake of a given magnitude (≤ Maximum Credible Earthquake) along a given fault, with a given probability ($P_n$) of occurring during a particular period of time may be estimated as follows:

$$T_m = \left(1 - T\sqrt{1 - P_n}\right)^{-1} \quad \text{.....(1)}$$

$P_n$ represents not only the probability of occurrence of a given magnitude along a given fault, but also the risk of occurrence of the associated ground motions. As the time scale for urban planning is in the order of a few decades, a return period commonly considered is 475 years, which corresponds to 10% probability of exceedance within 50 years. Other return periods may be considered according to the service life of a structure.

In this Study, we consider a 475-year return period, i.e. 10% probability of exceedance within 50 years. We also provide curves of magnitude versus mean return period for critical seismogenic sources in the Algiers area.

(B) Recurrence of Seismicity from Critical Seismogenic Sources

The seismic parameters that characterize each area are defined by the frequency distribution law or recurrence curve for the different earthquake sizes in each area. This distribution was defined by Gutenberg and Richter (1944) and assumes that the number of earthquakes (N) decreases exponentially with its magnitude (M), according to the following formula:

$$\log_{10} N(M) = a - b \cdot M \quad \text{.....(2)}$$

where N(M) is the number of earthquakes greater than M, "a" is the annual earthquake rate of a magnitude greater than 0 in the region, and "b" is the value which defines the relative ratio of large to small earthquakes. This equation assumes that all earthquakes are independent of space and time, i.e. it has the properties of a Poisson model. Several b-values are proposed in the literature, as listed in Table 5-2 below:

Table 5-2 Regional b-values Proposed in the Literature for Northern Algeria

| Reference | b-value |
|---|---|
| Hamdache, 1998 | 0.63 |
| Lopez Casado et al., 1995 | 0.77 |
| Geomatrix, 1998 | 0.32 to 0.35 |

It is assumed that all individual active faults could have a b-value equal to the regional b-value and for the purpose of the Study the regional b-value calculated by Hamdache (1998), i.e. 0.63, was adopted.

(C) Estimates of Magnitude versus Mean Return Period

The seismic moment, Mo, is the most physically meaningful parameter to describe the size of an earthquake in terms of static fault parameters:

$$Mo = \mu \cdot A_r \cdot D \quad \text{.....(3)}$$

where μ is the rigidity or shear modulus (usually taken as 3 x $10^{11}$ dyne/$cm^2$), $A_r$ is the rupture area on the fault plane undergoing slip during the earthquake, and D is

the average displacement over the slip surface. The total seismic moment rate, $\dot{M}o^T$, or the rate of seismic energy release along a fault is estimated by:

$$\dot{M}o^T = \mu \cdot A_f \cdot S \quad \text{.....(4)}$$

where S is the average slip rate along the fault and $A_f$ is the total fault plane area. The seismic moment rate provides an important link between geological and seismicity data. Seismic moment is translated to earthquake magnitude according to an expression of the form:

$$\log Mo = c \cdot m + d \quad \text{.....(5)}$$

The moment magnitude, m, is considered to be equivalent to the local magnitude within the range $3 < M_L < 7$ and to the surface wave magnitude within the range $5 < Ms < 7.5$.

Once the fault slip rate is used to constrain the seismic moment rate on the fault, a model must be assumed that describes how the rate of moment release is distributed to earthquakes of various magnitudes. Several authors have developed relationships between earthquake recurrence parameters and fault or crustal deformation rates, assuming an exponential magnitude distribution.

The link between fault slip rate and earthquake rates is made through the use of seismic moment. The total rate of seismic moment can be related to earthquake occurrence rate by the expression:

$$\dot{M}o^T = \int_{-\infty}^{m^u} \dot{n}(m) \cdot Mo(m) \cdot dm \quad \text{.....(6)}$$

where n(m) is the density function for earthquake occurrence rate and may be expressed according to Youngs and Coppersmith (1985) as :

$$n(m) = \frac{N(m^0)\beta \exp(-\beta(m - m^0)}{1 - \exp(-\beta(m^u - m^0))} \quad \text{for } m \le m^u \quad \text{.....(7)}$$

$N(m^o)$ is the normalised number of events per unit time, $m^u$ is the upper bound magnitude ($n(m) = 0$ for $m > m^u$), $m^o$ is some arbitrary reference magnitude, $\beta = b \times \ln 10$ with b from the Gutenberg-Richter exponential frequency magnitude relationship $\log N(m) = a - b \times m$, when N(m) is the cumulative number of earthquakes of magnitude greater than m, and a and b are constants.

Integrating equation (6), one obtains the reference magnitude corresponding to a given return period as a function of the upper bound magnitude, $m^u$, the associated upper bound seismic moment, the assumed slip-rate along the fault, the chosen return period, the b-value from the Gutenberg-Richter exponential frequency magnitude relationship, and the total fault plane area.

$$\mu \cdot A_f \cdot S = b\dot{N}(m^0) Mo^u \exp(-\beta(m^u - m^0)) / (c - b)(1 - \exp(-\beta(m^u - m^0))) \quad \text{.....(8)}$$

which is equivalent to the relationship developed by Anderson (1979) and the second-type relationship presented by Anderson and Luco (1983). The term $M_0^u$ is the moment for the upper bound magnitude $m^u$. Assuming that slip rate S on a fault is known, equation (8) provides a constraint on the three parameters of the recurrence relationship: $N(m^o)$, b and $m^u$.

The constraint imposed by fault slip rate allows the development of fault-specific recurrence relationships in regions where the historical seismicity data are only sufficient to establish the regional recurrence rate for small to moderately-sized earthquakes. For each fault in the region, estimates of the upper bound magnitude $m^u$ can be made using fault characteristics. The historical seismicity data can be used to determine a regional b-value. Assuming that individual faults all have a b-value equal to the regional b-value, the earthquake activity rate for each fault, $N(m^o)$, can be computed from the estimated slip rate for the fault using equation (8).

Hereafter, the reference magnitudes along each identified active faults are estimated taking into account the return period of the reference earthquakes ($N(m^o) = 1/T_m$), the slip-rate along the faults, the maximum seismogenic capability of the faults and the b-value.

$$m^0 = m^u - \frac{1}{b \cdot \ln 10} \ln\left[1 + \frac{N(m^0) b Mo^u}{(1.5 - b)\mu A_f S}\right] \quad \text{.....(9)}$$

where $Mo^u$ is the seismic moment corresponding to the maximum credible magnitude along a given fault.

2) Magnitude versus Mean Return Period for Critical Seismogenic Sources in the Algiers Area

Table 5-3 below summarizes the magnitudes associated with a 475 year return period for each critical seismogenic source and the parameters, deduced from the seismogenic context, that were used to estimate these magnitudes. Curves of magnitude versus mean return period are shown in Figure 5-8.

Table 5-3 Magnitudes Associated with 475 Year Return Period for Critical Seismogenic Sources in the Algiers Area

| Seismic Source | Upper Bound Magnitude (Mw) | Rupture Area ($km^2$) | Slip Rate (mm/yr) | Mw for 475 yr return period |
|---|---|---|---|---|
| Sahel Fault | 7.2 ± 0.3 | 1590 ± 210 | 0.5 ± 0.2 | 5.9 ± 0.3 |
| Chenoua Fault | 7.0 ± 0.3 | 1060 ± 210 | 0.5 ± 0.2 | 5.8 ± 0.3 |
| Blida Fault | 7.4 ± 0.3 | 2545 ± 280 | 2.5 ± 1.0 | 6.8 ± 0.2 |
| Khair al Din Fault | 7.4 ± 0.3 | 2830 ± 565 | 2.5 ± 1.0 | 6.8 ± 0.2 |
| Zemmouri Fault | 7.4 ± 0.3 | 2830 ± 565 | 4.0 ± 1.0 | 7.0 ± 0.1 |
| Thenia Fault | 6.8 ± 0.3 | 600 ± 150 | 0.75 ± 0.25 | 5.9 ± 0.2 |

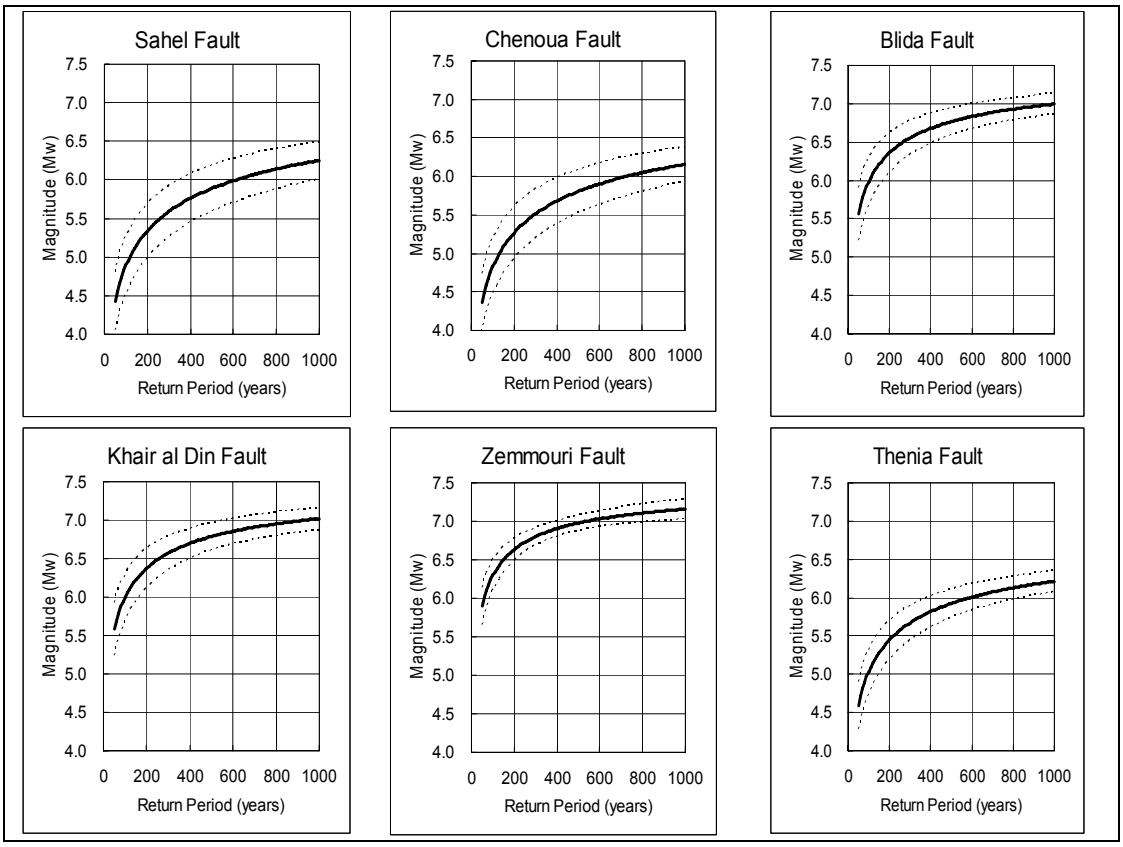


Figure 5-8 Magnitude vs Mean Return Period ; dashed lines show uncertainties (1σ)

[References]

Anderson J. G., 1979, Estimating the seismicity from geological structure for seismicrisk studies, Bull. Seism. Soc. Am. 71, 827-843.

Anderson J. G. and Luco J. E., 1983, Consequences of slip rate constraints on earthquake occurrence relations, Bull. Seism. Soc. Am. 73, 471-496.

Aymé A., 1952, Le quaternaire littoral des environs d'Alger, Actes du Cong. Panaf. De Préhistoire, II session, Alger 1952, 243-246.

Boudiaf A., 1996, Etude sismotectonique de la région d'Alger et de la Kabylie, (Algérie) : Utilisation des modèles numériques de terrains, (MNT) et de la télédétection pour la reconnaissances des structures tectoniques actives ; contribution à l'évaluation de l'aléa sismique, Thèse de Doctorat, Univ. Scien. Tech. Languedoc, France, 274 pp.

Bounif A., C. Dorbath, M. Meghraoui, H. Beldjoudi, N. Laouami, M. Frogneux, A. Slimani, P. J. Alasset, A. Kharoubi, F. Ousadou, M. Chik, A. Harbi, S. Larbes and S. Maouche, 2004. The 21 May, 2003, Zemmouri, (Algeria) earthquake Mw=6. 8 : Relocation and aftershock sequence analysis, Geoph. Res. Lett., 31, L19606, doi:10.1029/2004GL020586.

Deverchère J., Yelles K., Domzig A., Mercier de Lepinay B., Bouillin J.P., Gaullier V., Bracène R., Calais E., Savoye B., Kherroubi A., Le Roy P., Pauc H., and Dan G., 2005. Active thrust faulting offshore Boumerdes, Algeria, and its relation to the 2003 Mw 6.9 earthquake. Geophysical Research Letters, v. 32, L04311

Domzig A., Le Roy C., Yelles K., Deverchère J., Bouillin J-P., Bracene R., Mercier de Lèpinay B., Le Roy P., Calais E., Kherroubi A., Gaullier V., Savoye B., and Pauc H, submitted. Africa-Eurasia Miocene collision and neotectonics offshore Algeria: Preliminary results from the MARADJA cruise. Under review for publication in C.R. Géosciences (July 2005).